Remarkably Robust and Correlated Coherence and Antiferromagnetism in $(Ce_{1-x}La_x)Cu_2Ge_2$

H. Hodovanets,[1,2] S. L. Bud'ko,[1,2] W. E. Straszheim,[1] V. Taufour,[1,2] E. D. Mun,[2] H. Kim,[2] R. Flint,[1,2] and P. C. Canfield[1,2]
[1]*Ames Laboratory, Iowa State University, Ames, Iowa 50011, USA*
[2]*Department of Physics and Astronomy, Iowa State University, Ames, Iowa 50011, USA*
(Received 3 December 2014; revised manuscript received 20 April 2015; published 8 June 2015)

We present magnetic susceptibility, resistivity, specific heat, and thermoelectric power measurements on $(Ce_{1-x}La_x)Cu_2Ge_2$ single crystals ($0 \leq x \leq 1$). With La substitution, the antiferromagnetic temperature T_N is suppressed in an almost linear fashion and moves below 0.36 K, the base temperature of our measurements for $x > 0.8$. Surprisingly, in addition to robust antiferromagnetism, the system also shows low temperature coherent scattering below T_{coh} up to ~0.9 of La, indicating a small percolation limit ~9% of Ce. T_{coh} as a function of magnetic field was found to have different behavior for $x < 0.9$ and $x > 0.9$. Remarkably, $(T_{coh})^2$ at $H = 0$ was found to be linearly proportional to T_N. The jump in the magnetic specific heat δC_m at T_N as a function of T_K/T_N for $(Ce_{1-x}La_x)Cu_2Ge_2$ follows the theoretical prediction based on the molecular field calculation for the $S = 1/2$ resonant level model.

DOI: 10.1103/PhysRevLett.114.236601 PACS numbers: 72.15.Qm, 75.20.Hr, 75.30.Kz, 75.30.Mb

Dilution studies of the Kondo lattice provide a unique probe to understand the interrelation between Kondo coherence and magnetic order. In a dilution study of the antiferromagnetically (AFM) ordered Kondo lattice $(Ce_{1-x}La_x)Cu_2Ge_2$, we find a remarkably wide region of antiferromagnetic order and Kondo coherence up to $x = 0.8$ and $x = 0.9$, respectively, along with an unexpected scaling of $T_N \sim (T_{coh})^2$. This wide region appears to contradict current theoretical predictions for Kondo coherence alone, which state that coherence vanishes for much smaller x [1], giving rise to either a broad region of non-Fermi liquid [2] or a Lifshitz transition [3,4]. Our findings suggest that, in this system, magnetic correlations actually reinforce the Kondo coherence.

As a result of competition between the Kondo effect and Ruderman-Kittel-Kasuya-Yosida (RKKY) interaction, Kondo lattices display a variety of ground states (long-range magnetic order, unconventional superconductivity, non-Fermi liquid, etc. [5–8]) and are characterized by multiple energy scales (antiferromagnetic T_N or superconducting T_c ordering temperature, the single-ion Kondo temperature T_K, the coherence temperature T_{coh}, and the crystal electric field (CEF) splitting). Ce-based compounds, both in coherent and diluted regimes, have been studied for more than four decades with the hope of understanding how coherence develops with an increase of the Kondo impurity concentration (Refs. [9–17] and references therein). For example, $(Ce_{1-x}La_x)Pb_3$ shows coherence up to $x = 0.15$ and single-ion Kondo scaling for a surprisingly wide range of x and T (T_K is the same for these concentrations) [12,18]. In the study of $(Ce_{1-x}La_x)Ni_2Ge_2$, the coherence was found up to $x = 0.4$ with impressive single-ion Kondo scaling in the coherent Fermi liquid as well as diluted regimes [17].

Based on analysis of La dilution of $CeCoIn_5$ (for which T_K, T_{coh}, and CEF are well separated), a two-fluid description of the Kondo lattice was put forward [19]. It proposes two different energy scales for the Kondo lattice: characteristic temperature T^* ($T^* = T_{coh}$ for nondiluted, parent compound) that governs the intersite coupling of the f shells in the coherent Kondo lattice and the concentration-independent single-ion T_K, responsible for the on-site $4f$- conduction-electron hybridization. T_{coh} for this system was observed up to $x \sim 0.4$ [16].

In this work, we study La dilution of the Kondo lattice compound $CeCu_2Ge_2$ where $T_N \sim 4$ K [20–22] and the two excited CEF levels at $\Delta E_1 \sim 197$ K and $\Delta E_2 \sim 212$ K [23] are well separated from the ground state doublet. The measurements were performed on single crystals grown by the high temperature flux method [24–26]. The actual concentrations of La or Ce were assessed by wavelength dispersive x-ray spectroscopy (WDS) and the results of the Curie-Weiss fits of the temperature dependent susceptibility. The WDS values of La/Ce concentrations will be used throughout the text if not specified otherwise. La concentrations will be denoted by x and Ce concentrations will be denoted by $y = 1 - x$ to avoid confusion. The details of samples growth, evaluation of La concentrations, and measurement techniques can be found in the Supplemental Material [27].

An almost classic, mean-field-like second order AFM transition is clearly seen in the specific heat $C_p(T)$ data for $CeCu_2Ge_2$ (Fig. 1). As the amount of La is increased, the AFM transition moves to lower temperature and is still clearly observable for $x = 0.80$. When T_N is suppressed enough, in addition to the AFM ordering, a broad maximum appears in the specific heat data starting from $x = 0.75$ (inset to Fig. 1), the position of which shifts

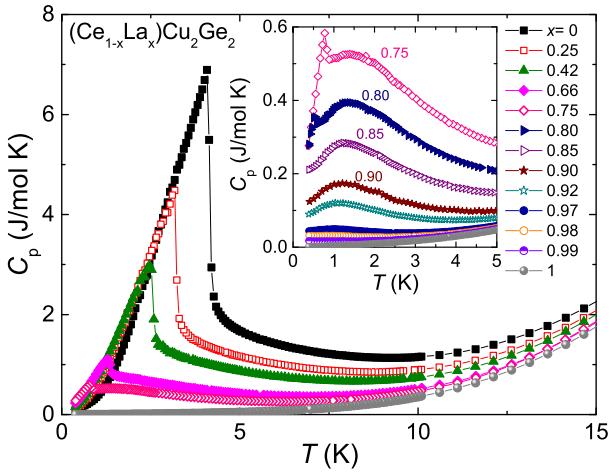

FIG. 1 (color online). Specific heat $C_p(T)$ data of $(Ce_{1-x}La_x)Cu_2Ge_2$ single crystals. The inset shows enlarged low-temperature data for $0.75 \leq x \leq 1$. The data for $x = 0.75$ are shown in both graphs for clarity.

slightly to lower temperatures as the La concentration is further increased. The maximum becomes almost indiscernible for $x = 0.99$. This maximum is associated with the Kondo temperature T_K of a single-ion Kondo impurity ($T_K > T_N$) [27].

A hallmark of the single-ion Kondo effect is the minimum and lower-temperature logarithmic dependence of the resistivity data. The zero-field, temperature dependent, in-plane, resistivity $\rho(T)$ data of $(Ce_{1-x}La_x)Cu_2Ge_2$ are shown on a semilogarithmic plot in Fig. 2. For $CeCu_2Ge_2$, the $\rho(T)$ data exhibit a broad maximum at ~100 K associated with a thermal depopulation of the exited CEF levels as the temperature is decreased. At lower temperatures, the $\rho(T)$ plot shows a second broad maximum corresponding to a crossover from incoherent to coherent scattering of the electrons on the magnetic moments at $T_{coh} \sim 5.5$ K, characteristic of that of Kondo lattice compounds. The maximum is followed by (and actually truncated by) a kink corresponding to the AFM transition. As the amount of La is increased, the AFM transition moves to lower temperatures. The kink, corresponding to the AFM transition, becomes less discernible. Most intriguingly, the truncated maximum, at T_{coh} for $CeCu_2Ge_2$, evolves into a broad maximum and remains present up to $x = 0.90$, Fig. 2(b). For $x = 0.92$, the resistivity data tend to saturation at the lowest temperature measured. This behavior in the resistivity is reminiscent of the single-ion Kondo impurity. For the three smallest Ce concentrations, the resistivity data display the minimum followed by a $-\log(T)$ dependence upon cooling to the lowest temperature. It is worth pointing out that the slightly temperature dependent minimum at ~20 K in the resistivity data is observed for all samples containing Ce. T_{min} is proportional to the concentration of Ce, $y^{1/5}$, only for $0.01 \leq y \leq 0.08$ (see the Supplemental Material

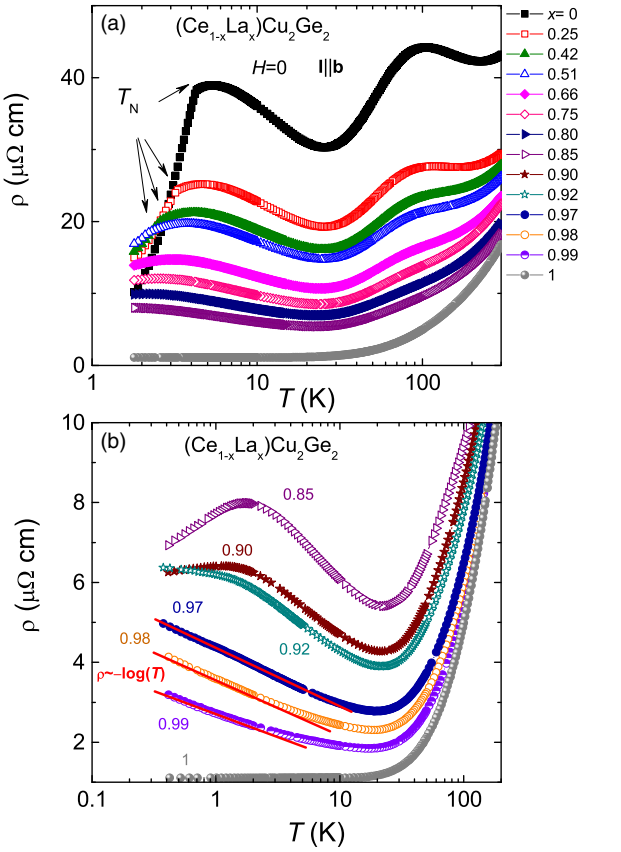

FIG. 2 (color online). (a) and (b) The zero-field, in-plane (I||**b**), temperature-dependent resistivity $\rho(T)$ data of $(Ce_{1-x}La_x)Cu_2Ge_2$ single crystals on a semilogarithmic plot. The data for $x = 0.85$ is shown in both panels for continuity.

[27]) consistent with the single-ion Kondo impurity effect.

Thermoelectric power (TEP) can also provide information about the T_{coh} and T_K characteristic energy scales. Temperature-dependent thermoelectric power $S(T)$ data for $(Ce_{1-x}La_x)Cu_2Ge_2$ single crystals are shown in Fig. 3. The broad peak observed for $LaCu_2Ge_2$ at ~75 K ($\sim 0.2 \times \Theta_D$) is probably due to the phonon drag contribution expected at $0.1–0.3\Theta_D$ [27,37]. For all samples containing Ce, a broad, high-T maximum due to (i) the thermal depopulation of the two excited CEF doublets [23] as the temperature is lowered and (ii) possibly phonon drag contribution, is observed around 100 K. Since the energy separation between those two excited CEF levels is small, only one maximum at high temperatures is seen in the TEP measurements. The position of this maximum is almost unaffected by La substitution.

The TEP data of $LaCu_2Ge_2$ are positive over the whole temperature range measured. However, 0.01 of Ce is enough to change the functional dependence of the TEP below ~24 K: the TEP for $x = 0.99$ crosses zero twice by going through a low-T minimum and has a low-T maximum at ~0.6 K (see inset to Fig. 3). Such TEP behavior is

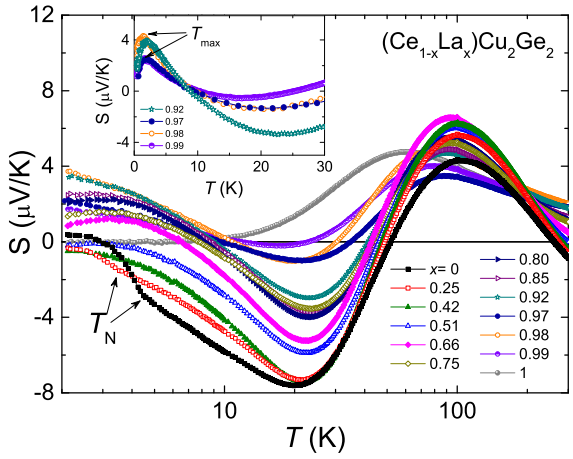

FIG. 3 (color online). The zero-field, temperature-dependent thermoelectric power $S(T)$ of $(Ce_{1-x}La_x)Cu_2Ge_2$ single crystals. $S(T)$ of $(Ce_{1-x}La_x)Cu_2Ge_2$ $(0.92 \leq x \leq 1)$ single crystals at lower temperatures is shown in the inset. $\nabla T \| \mathbf{b}$.

expected for the Ce single-ion Kondo impurity [38–40]. For the highly La diluted samples, this low-temperature maximum is believed to correspond to the single-ion impurity Kondo temperature T_K. As the amount of Ce is increased, the absolute value of $S_{\min}$ increases as well probably reflecting the amount of Ce ions and increased scattering associated with the increase of Ce.

The $T - x$ phase diagram for $(Ce_{1-x}La_x)Cu_2Ge_2$, Fig. 4, shows the characteristic temperatures and energy scales as a function of La concentration. T_N (as determined from specific heat, magnetization, resistivity and TEP measurements) decreases almost linearly with x and moves below

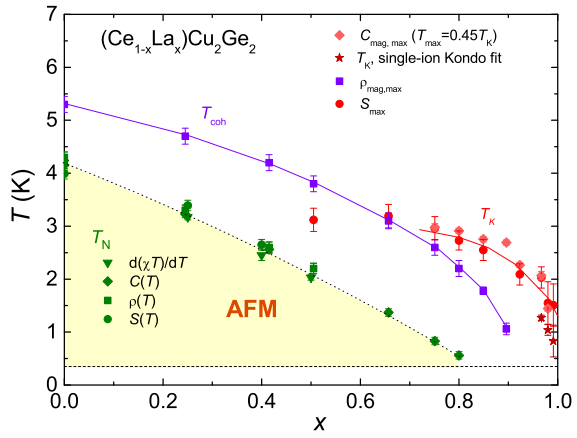

FIG. 4 (color online). $T - x$ phase diagram for $(Ce_{1-x}La_x)Cu_2Ge_2$ single crystals. Lines are guides to the eye. The horizontal line at 0.36 K is the lowest base temperature of the measurements. The data for magnetization measurements and T_K values, estimated using Schotte and Schotte model of the specific heat data, can be found in the Supplemental Material [27]. Kondo temperature T_K was also estimated from the specific heat data by using $T_{\max} = 0.45\ T_K$ criterion [41] (see text for details).

the base temperature of 0.36 K or disappears for $x > 0.80$ and $T_{\rm coh}$ extends down to $x = 0.90$. The low-temperature maxima in the TEP data seem to coincide with the T_K values estimated from the specific heat data using a $T_{\max} = 0.45\ T_K$ criterion [41] rather well, here $T_{\max}$ is the temperature where the maximum occurs. The T_K values estimated using the Schotte and Schotte single-ion Kondo model fit [27,42] of the specific heat data although lower, are still within the error bars of the ones estimated using the $T_{\max} = 0.45\ T_K$, criterion. The decrease of the Kondo temperature from ~4 K ($x = 0$) to ~1 K ($x = 0.99$) upon La substitution is consistent with the unit cell volume increase with x in terms of the Doniach phase diagram [43,44]; i.e., the system is tuned away from a quantum critical point (QCP). However, La substitution dilutes out the magnetic moment of the system which is not accounted for in the Doniach phase diagram.

Based on the molecular field calculations for the $S = 1/2$ resonant level model, a close relationship between the specific heat jump, δC_m, at the ordering temperature and the ratio between the two characteristic temperatures T_K and T_N for magnetic Ce and Yb Kondo systems with doublet ground states was found [45]. If the T_K values shown in Fig. 4 are used and T_K for $CeCu_2Ge_2$ assumed 4 K, $(Ce_{1-x}La_x)Cu_2Ge_2$ fits that description rather well, Fig. 5(a). This further supports the thought that the estimated T_K values are reasonable and the CEF ground state is a doublet.

The presence of the AFM transition and linear dependence of it on x to a high value of La is not unique to the $(Ce_{1-x}La_x)Cu_2Ge_2$ system. Such behavior of T_N upon La dilution was also observed in $(Ce_{1-x}La_x)Pd_2Si_2$ [13], as well as in $(Ce_{1-x}La_x)Au_2Si_2$, and $(Ce_{1-x}La_x)Ag_2Si_2$ [14]. The Ce-based parent compounds of these families, including $CeCu_2Ge_2$, order antiferromagnetically, with different ordering wave vectors, and belong to the same $I4/mmm$ space group of the tetragonal crystal structure. However, a progression of the $T_{\rm coh}$, that corresponds to the crossover from incoherent to coherent scattering, with La substitution was not commented on for these systems, perhaps because T_N and $T_{\rm coh}$ could not be well separated. In this respect, $(Ce_{1-x}La_x)Cu_2Ge_2$ appears to be a unique system—the $T_{\rm coh}$ is well separated from the AFM feature and extends all the way to ~0.9 of La.

Remarkably, $(T_{\rm coh})^2$ is linearly proportional to T_N, Fig. 5(b), over a wide range of x and both seem to go to zero at $x \sim 0.9$. As of yet, there is no theory to explain the clear and compelling dependence of $T_{\rm coh}$ on T_N.

In addition, a different field dependence of the $T_{\rm coh}$-value was found in the single-ion regime, Fig. 5(c), which also supports the conclusion that $y \leq 0.09$ defines the limit of the single ion regime in the zero-field limit (Fig. 5(c) is based on the data given in the Supplemental Material [27]). The functional dependence of $T_{\rm coh}$ on H for $x = 0.92$ is clearly different from that for smaller La concentrations;

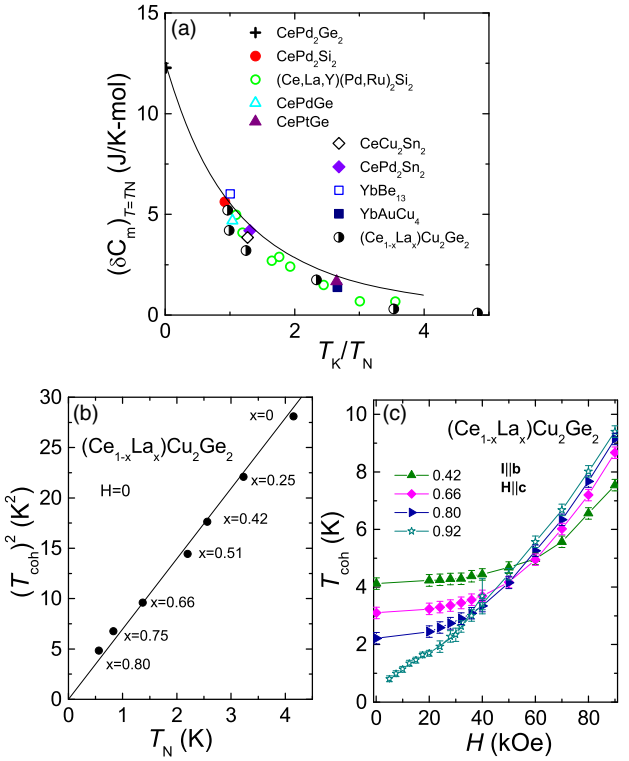

FIG. 5 (color online). (a) Variation of the jump in the specific heat δC_m at the magnetic transition as a function of T_K/T_N. The data for the compounds not studied in this work together with the solid curve were digitized from Ref. [45]. Solid line is the calculated specific heat jump at the T_N for a doublet ground state system [45]. (b) $(T_{\rm coh})^2$ as a function of T_N. Solid line is a guide to the eye. (c) $T_{\rm coh}$ as a function of H (based on $\rho(T)$ at constant H data given in the Supplemental Material [27]).

i.e., for $x < 0.9$, $T_{\rm coh}$ saturates to a finite value as $H \to 0$, and this is not the case for the $x = 0.92$ data. Also, for $x = 0.92$, there is no $T_{\rm coh}$ at $H = 0$ and $T_{\rm coh}$ is induced by magnetic field for all applied fields as opposed to smaller La concentrations.

This dilution study raises a number of questions or challenges for theories of the Kondo lattice. In particular, why do T_N and $T_{\rm coh}$ persist out to 90% La substitution? And why does T_N scale as $(T_{\rm coh})^2$? In a simple percolation picture, this persistence indicates that the Kondo lattice has a low percolation threshold, consistent with a three-dimensional network with further neighbors; e.g., the cubic lattice with second and third neighbor interactions has a percolation threshold of 0.0976 [46,47]. Once coherence is established, the system can develop an AFM transition. At a more qualitative level, given that the clear AFM ordering signatures persist out to $x = 0.8$, indicating that there is clear coupling and interaction between the remains of the Ce-sublattice, it is not at all surprising that this same coupling and interactions support coherence between ions. More sophisticated numerical studies of the dilute Kondo lattice give a crossover between coherent and single-ion Kondo behaviors at $x \approx 0.1$ only for very low conduction electron carrier densities, $n_c \ll 1$ [2,4]. There are no experimental indications that n_c for $CeCu_2Ge_2$ is so small, and this is contraindicated by the observation that $T_{\rm coh} > T_K$ [48] and by band structure calculations [49]. The large discrepancy between these numerical studies and our results suggests that large intersite correlations are essential to Kondo coherence in the dilute limit of $(Ce_{1-x}La_x)Cu_2Ge_2$, unlike in other materials such as $(Ce_{1-x}La_x)CoIn_5$ [16,19] and $(Ce_{1-x}La_x)Pb_3$ [12,18]. The unusual scaling of T_N with $(T_{\rm coh})^2$ is unexpected and counters results of the two-fluid model, where T^* and T_N are expected to behave similarly [19].

In summary, La substitution drives T_N in a roughly linear fashion from ~4 K (for $x = 0$) to below 0.36 K, the base temperature of our measurements, for $x > 0.8$. However, $T_{\rm coh}$, corresponding to the crossover from incoherent to coherent scattering, was observed up to $x \sim 0.9$. This indicates that the percolation limit of the lattice of Ce ions is rather small and implies the 3D nature of the Kondo "clouds." No non-Fermi liquid or Fermi liquid behavior that would indicate a quantum critical point was observed in the thermodynamic and transport measurements upon suppression of T_N. We find $y \leq 0.09$ is the single ion regime with $T_{\rm coh}$ showing different behavior as a function of H for $x > 0.9$ and $x < 0.9$. Remarkably, $(T_{\rm coh})^2$ at $H = 0$ was found to be linearly proportional to T_N over a wide range of x. $(Ce_{1-x}La_x)Cu_2Ge_2$ appears to be the only system where $T_{\rm coh}$ is observed down to $x = 0.9$ of La, $T_{\rm coh}$ is well separated from magnetic ordering and single impurity effects, and $T_{\rm coh}$ shows a parabolic dependence on T_N. Our results indicate that $(Ce_{1-x}La_x)Cu_2Ge_2$ is a particularly compelling system and may be very useful for understanding the Kondo and RKKY effects.

The authors would like to thank J. Schmalian, P. Riseborough, Z. Fisk, B. C. Sales, J. D. Thompson, and F. Steglich for insightful discussions. This work was supported by the U.S. Department of Energy (DOE), Office of Science, Basic Energy Sciences, Materials Science and Engineering Division. The research was performed at the Ames Laboratory, which is operated for the U.S. DOE by Iowa State University under Contract # DE-AC02-07CH11358. E. D. M and H. K. were supported by the AFOSR-MURI Grant No. FA9550-09-1-0603.

[1] Z. Tešanović, Phys. Rev. B **34**, 5212 (1986).
[2] R. K. Kaul and M. Vojta, Phys. Rev. B **75**, 132407 (2007).
[3] I. M. Lifshitz, Sov. Phys. JETP **11**, 1130–1135 (1960).
[4] S. Burdin and C. Lacroix, Phys. Rev. Lett. **110**, 226403 (2013).
[5] G. R. Stewart, Rev. Mod. Phys. **56**, 755 (1984).
[6] G. R. Stewart, Rev. Mod. Phys. **73**, 797 (2001).
[7] G. R. Stewart, Rev. Mod. Phys. **78**, 743 (2006).

[8] O. Stockert and F. Steglich, Annu. Rev. Condens. Matter Phys. **2**, 79 (2011).
[9] K. Samwer and K. Winzer, Z. Phys. B **25**, 269 (1976).
[10] C. Bredl, F. Steglich, and K. Schotte, Z. Phys. B **29**, 327 (1978).
[11] W. Felsch, Z. Phys. B **29**, 211 (1978).
[12] C. L. Lin, A. Wallash, J. E. Crow, T. Mihalisin, and P. Schlottmann, Phys. Rev. Lett. **58**, 1232 (1987).
[13] E. V. Sampathkumaran, Y. Nakazawa, M. Ishikawa, and R. Vijayaraghavan, Phys. Rev. B **40**, 11452 (1989).
[14] C. J. Garde and J. Ray, J. Phys. Condens. Matter **6**, 8585 (1994).
[15] A. C. Hewson, *The Kondo Problem to Heavy Fermions*, 2 (Cambridge University Press, Cambridge, England, 1997).
[16] S. Nakatsuji, S. Yeo, L. Balicas, Z. Fisk, P. Schlottmann, P. G. Pagliuso, N. O. Moreno, J. L. Sarrao, and J. D. Thompson, Phys. Rev. Lett. **89**, 106402 (2002).
[17] A. P. Pikul, U. Stockert, A. Steppke, T. Cichorek, S. Hartmann, N. Caroca-Canales, N. Oeschler, M. Brando, C. Geibel, and F. Steglich, Phys. Rev. Lett. **108**, 066405 (2012).
[18] P. Schlottmann, Phys. Rep. **181**, 1 (1989).
[19] S. Nakatsuji, D. Pines, and Z. Fisk, Phys. Rev. Lett. **92**, 016401 (2004).
[20] U. Rauchschwalbe, U. Gottwick, U. Ahlheim, H. Mayer, and F. Steglich, J. Less-Common Met. **111**, 265 (1985).
[21] R. Felten, G. Weber, and H. Rietschel, J. Magn. Magn. Mater. **63–64**, 383 (1987).
[22] F. de Boer *et al.*, J. Magn. Magn. Mater. **63–64**, 91 (1987).
[23] M. Loewenhaupt, E. Faulhaber, A. Schneidewind, M. Deppe, and K. Hradil, J. Appl. Phys. **111**, 07E124 (2012).
[24] P. C. Canfield and Z. Fisk, Philos. Mag. B **65**, 1117 (1992).
[25] P. C. Canfield, in *Book on Complex Metallic Alloys* (World Scientific, Singapore, 2010), Vol. 2, Chap. 2, pp. 93–111.
[26] P. C. Canfield and I. R. Fisher, J. Cryst. Growth **225**, 155 (2001).
[27] See Supplemental Material at http://link.aps.org/supplemental/10.1103/PhysRevLett.114.236601 for more details on (i) sample preparation, thermodynamic and transport measurements, and (ii) data analysis, which includes Refs. [28–36].
[28] http://www.qdusa.com/sitedocs/appNotes/mpms/1014-201.pdf.
[29] E. Mun, S. L. Bud'ko, M. S. Torikachvili, and P. C. Canfield, Meas. Sci. Technol. **21**, 055104 (2010).
[30] H. Hodovanets, S. L. Bud'ko, X. Lin, V. Taufour, M. G. Kim, D. K. Pratt, A. Kreyssig, and P. C. Canfield, Phys. Rev. B **88**, 054410 (2013).
[31] J. A. Mydosh, *Spin Glasses: An Experimental Introduction* (Taylor & Francis, London, 1993).
[32] P. Schlottmann, J. Magn. Magn. Mater. **52**, 214 (1985).
[33] H. Gruhl and K. Winzer, Solid State Commun. **57**, 67 (1986).
[34] K. Satoh, T. Fujita, Y. Maeno, Y. Ōnuki, and T. Komatsubara, J. Phys. Soc. Jpn. **58**, 1012 (1989).
[35] V. T. Rajan, J. H. Lowenstein, and N. Andrei, Phys. Rev. Lett. **49**, 497 (1982).
[36] J. Ruvalds and Q. G. Sheng, Phys. Rev. B **37**, 1959 (1988).
[37] F. J. Blatt, P. A. Schroeder, C. L. Foiles, and D. Greig, *Thermoelectric Power of Metals* (Plenum Press, New York, 1976).
[38] V. Zlatić, B. Horvatić, I. Milat, B. Coqblin, G. Czycholl, and C. Grenzebach, Phys. Rev. B **68**, 104432 (2003).
[39] V. Zlatić and R. Monnier, Phys. Rev. B **71**, 165109 (2005).
[40] V. Zlatić, R. Monnier, J. K. Freericks, and K. W. Becker, Phys. Rev. B **76**, 085122 (2007).
[41] H.-U. Desgranges and K. Schotte, Phys. Lett. **91A**, 240 (1982).
[42] K. D. Schotte and U. Schotte, Phys. Lett. **55A**, 38 (1975).
[43] S. Doniach, Physica (Amsterdam) **91B+C**, 231 (1977).
[44] P. Coleman, in *Handbook of Magnetism and Advanced Magnetic Materials* (John Wiley & Sons, New York, 2007), Vol. 1, pp. 95–148.
[45] M. Besnus, A. Braghta, N. Hamdaoui, and A. Meyer, J. Magn. Magn. Mater. **104–107**, Part 2, 1385 (1992).
[46] C. Domb and N. W. Dalton, Proc. Phys. Soc. **89**, 859 (1966).
[47] L. Kurzawski and K. Malarz, Rep. Math. Phys. **70**, 163 (2012).
[48] S. Burdin, A. Georges, and D. R. Grempel, Phys. Rev. Lett. **85**, 1048 (2000).
[49] G. Zwicknagl, J. Low Temp. Phys. **147**, 123 (2007).